Supporting Information

Hydrogen Bonds and Ionic forms Versus Polymerization of Imidazole at High Pressures

Bharat Bhooshan Sharma, Ashok K. Verma, Susy Thomas, Chitra Murli*, Surinder M. Sharma

High Pressure & Synchrotron Radiation Physics Division, Bhabha Atomic Research Centre, Mumbai- 400 085, India

Methods

Raman spectroscopy

Polycrystalline sample of imidazole purchased from Sigma-Aldrich Company was loaded in a hole of diameter ~100 μm drilled in a pre-indented stainless steel gasket of thickness ~60 μm in a Mao-Bell type diamond anvil cell. High pressure Raman spectra were collected in the back scattering geometry using single stage Jobin-Yvon HR460 spectrograph (resolution 4 cm^{-1}) with Liquid Nitrogen cooled CCD. Diode pumped solid state laser of 532 nm wavelength was used as excitation source. Pressure was monitored by R-lines of ruby fluorescence. Experiments were carried out without any pressure transmitting medium in order to avoid interaction of the sample with the medium. The lattice region 50-200 cm^{-1} of imidazole under ambient conditions was recorded using T64000 spectrograph. The observed spectral changes at higher pressures are likely to be intrinsic rather than due to non-

* To whom correspondence to be addressed; Tel.:91-22-25591326; Fax: 91-22-25505296. Email: cmurli@barc.gov.in (C. M.)

hydrostatic effect as there was no significant increase in the line width of ruby R-lines, which indicates that sample itself acts as a soft medium.

Ab-initio calculations

The density functional theory based *ab-initio* calculations were performed using Vienna *ab initio* Simulation Package (VASP).[1-4] The exchange-correlation functional was treated with the generalized gradient corrected scheme of Perdew-Burke-Ernzerhof.[1] The interactions between valence electrons and core were treated within the frozen-core all electron projector-augmented-wave (PAW) approach and plane wave basis set was constructed using an energy cut-off of 500 eV. The Brillouin zone (*BZ*) integrations were carried out using a uniform 6×6×4 Monkhorst-Pack ***k***-point grid. All free parameters of crystal lattice were optimized as a function of volume. The Raman spectra were calculated using the density functional perturbation theory as implemented in the Quantum-Espresso computer code.[5] For these calculations we have used the local density approximation for exchange-correlation[6] since code does not allow GGA calculations. An energy cutoff of 160 Ry was used for plane wave expansion. The Brillouin zone was sampled using same Monkhorst-Pack ***k***-point grid as in structural relaxations. The crystal structures were fully optimized before these calculations.

Results

Raman spectroscopy

Imidazole under ambient conditions is well characterized by Raman, infra-red, theoretical and inelastic neutron scattering methods.[7-18] Imidazole molecule ($C_3H_4N_2$) has (3 x 9) – 6 = 21 vibrational internal modes with C_s point group symmetry. Out of 21 there are 15 in-plane vibrations (A′) and 6 are out-of-plane vibrations (A″). These internal modes include 4 stretching vibrations (Γ_{str} = 4 A′) three C-H, one N-H stretch and remaining 17 (Γ_{bend} = 11

A′+ 6 A″) are ring vibrations. In the monoclinic crystal structure ($P2_1/c$), there are 4 molecules per unit cell; hence there are 21 lattice vibrations (external modes) (6 A_g+ 6 B_g+ 5 A_u+ 4 B_u, where A_g, B_g are Raman active and A_u, B_u are IR active). Therefore, in total, there are 12 Raman active external modes and 42 Raman active internal modes out of which about 30 internal modes were observed at ambient conditions as well as at high pressures. The assignment of the observed modes are based on our ab-initio calculations and is consistent with that given in the earlier studies.[9-15]

We have recorded the Raman spectrum of imidazole at various pressures (0.1 MPa - 20 GPa) and on release in the spectral region of interest from 200-3500 cm^{-1} excluding the region 1300-1400 cm^{-1} where strong Raman mode of diamond exists. Figures 2, 3, 4 show the Raman spectra in the pressure range 0.2 – 5.2 GPa and 5.8 - 20.1 GPa respectively (main manuscript). Raman shift (in cm^{-1}) versus pressure curve of the observed Raman modes at different pressures are given in Figure 9.

Spectral region 100 - 400 cm^{-1}

Table 2 lists the observed lattice Raman modes at ambient conditions and at higher pressures. As high pressure experiments were carried out using single stage spectrograph, except for the mode at 148 cm^{-1} which was observed at ambient conditions, all the other modes became observable only at higher pressures. The extrapolation of their values from ambient conditions recorded using T64000 triple spectrograph (Table 2) suggests that they are the lattice modes which have stiffened under pressure and have become observable at higher pressures. The mode at 148 cm^{-1} shows relatively larger increase in the frequency ($d\nu/dP$ =27 cm^{-1}/GPa) compared to the other modes in this region. At pressures above ~10

GPa, the relative intensity of the mode close to ~196 cm^{-1} increases substantially with respect to the mode at 177 cm^{-1}(observed at 10 GPa) as can be seen in Figure 2 (see the main text).

Spectral region 600-1700 cm^{-1}

The Raman mode frequencies which showed increase with pressure in the pressure range of our study are R-pucker/C-H wag (623 cm^{-1}, 661 cm^{-1}, 742 cm^{-1}), 836 cm^{-1}(unassigned), C-H wag (924 cm^{-1}), N-H wag (930 cm^{-1}), C-H deformation (1060 $cm^{-1}$and 1066 cm^{-1}), 1097 cm^{-1} (unassigned), ring stretch/N-H deformation (1145 cm^{-1}), N-H bend (1178 cm^{-1}), C-H/N-H deformation (1186 cm^{-1}), ring stretch (1450 cm^{-1}) and ring deformation (1542 cm^{-1}) (Figure 9). The mode frequencies which decrease with pressure are C-H wag (830 cm^{-1}) and ring bend deformation (901 cm^{-1}). N-H deformation (1500 cm^{-1}), 1480 cm^{-1}(unassigned) softens up to 0.5 GPa and stiffens at higher pressures.

C-H wag (830 cm^{-1}) softens up to ~2.6 GPa and shows stiffening at higher pressures, while C-H deformation mode (1090 cm^{-1}) remains observable only up to ~ 5 GPa. As shown in Figure 2 (main text),the relative intensity of N-H bend (1178 cm^{-1}) and C-H/N-H deformation (1186 cm^{-1}) with respect to C-H wag (924 cm^{-1}) reduces with pressure and the rate of reduction is found to be higher at pressures above 10 GPa. At pressures above 8 GPa, reduction in the intensity and softening of NH deformational modes were noted. Across this pressure, new modes ~ 870 cm^{-1} and ~ 1160 cm^{-1} emerge and show increase in the relative intensity at higher pressures. At pressures above 10 GPa, new modes close to the ring stretch (shoulder peak 1480 cm^{-1}) and 1550 cm^{-1} emerge and the latter one shows pressure induced softening up to 15 GPa (Figure 3 in main text). Above this pressure, anomalous spectral changes such as appearance of relatively sharper mode around the ring stretch 1480 cm^{-1} riding over a broad band and disappearance of the new mode (1550 cm^{-1}) were noted.

Spectral region 3000-3400 cm^{-1}

At ambient conditions, three vibrational modes C1-H1 symmetric stretch (3123 cm^{-1}), C2-H2/C3-H3 asymmetric stretch (3125 cm^{-1}) and C2-H2/C3-H3 symmetric stretch (3145 cm^{-1}) modes of imidazole are observed (Figure 4 in main text). C1-H1 (3123 cm^{-1}) shows significant reduction in the relative intensity with respect to the C2-H2/C3-H3 (3145 cm^{-1}) in the pressure range 0.5 to 2.5 GPa. At ~ 1 GPa, a new mode emerges at ~ 3140 cm^{-1} which gets buried under the C2-H2/C3-H3 mode across 2.6 GPa. Above this pressure, its relative intensity with respect to C2-H2/C3-H3 mode increases with pressure and is well resolved at 5.2 GPa and observed at 3185 cm^{-1}. At ~ 6 GPa, another new mode, which is possibly due to splitting of C2-H2 and C3-H3 modes, emerges close to C2-H2/C3-H3 and becomes well resolved at higher pressures (Figure 4 of main text). The C2-H2/C3-H3 asymmetric stretching mode frequency continues to increase with pressure. Across ~ 15 GPa, a broad band with complex profile emerges around the CH stretching modes.

Ab initio calculations

The pressure induced variation of the lattice parameters and unit cell volume of imidazole up to 10 GPa are shown in Figure 10. The variation in the cell parameters up to 3 GPa is close to the values reported in the experimental single crystal x-ray diffraction study of imidazole.[19] The calculated bulk modulus using Birch-Murnaghan equation of state is ~ 9.8 GPa. The refined N-H bond length, N-H---N, C-H---N, C-H---C hydrogen bond lengths and angles and C-H bond lengths at various pressures are shown in Figure 6, 7 and Figure 8 (see main text). The vibrational modes of the crystalline imidazole have also been calculated at different volumes 367 $Å^3$ (0.1 MPa), 305 $Å^3$ (3.3 GPa) and 274 $Å^3$ (6.3 GPa) and are shown in Figure 5 (see main text).

Structural changes in the pressure range 0.1 MPa - 2.5 GPa

Based on single crystal x-ray diffraction study[19] on imidazole up to 3 GPa, an earlier report established the stability of α-phase up to 2.7 GPa. However a new polar **β** (orthorhombic) phase was shown to get isochorically recrystallized above 1.2 GPa at 500 K. It is also reported that at ~ 8-12 GPa, inter-molecular N---N distance would reduce to 2.554 Å for H atom to assume the centre position, which would facilitate H atom hopping. Our ab-initio calculations indicate non-monotonic changes in the N-H---N and some of the C-H---N and C-H---C parameters at 0.5 GPa suggesting subtle molecular rearrangements across this pressure. In the high pressure Raman spectra, reduction in the relative intensity of the C1-H1 stretching mode with respect to C2-H2/C3-H3 stretching mode are also noted. Across ~ 2.5 GPa, relative strengths of the calculated inter-layer and intra-layer bond parameters change considerably. This is due to relatively less variation in the compressibility along the ***c*** axis (intra-layer) with respect to ***a*** and ***b*** axis (inter-layer). The discontinuous changes in the Raman modes across ~ 2.5 GPa may therefore be due to variation in the intra-layer and inter-layer compression. Absence of any new spectral features indicate that there is no structural transformation across this pressure, which is consistent with the earlier single crystal x-ray diffraction study.[19]

References

1. Perdew, J. P.; Burke, K.; Ernzerhof, M. Generalized Gradient Approximation Made Simple. *Phys. Rev. Lett.* **1996**, *77*, 3865-3868.
2. Kresse, G.; Hafner, J. Norm-Conserving and Ultrasoft Pseudopotentials for First-Row and Transition Elements. *J. Phys.- Condens. Mat.* **1994**, *6*, 8245-8257.
3. Kresse, G.; Joubert, D. From Ultrasoft Pseudopotentials to the Projector Augmented-Wave Method. *Phys. Rev. B* **1999**, *59*, 1758-1775.
4. Blochl, P. E. Projector Augmented-Wave Method. *Phys. Rev. B* **1994**, *50*, 17953-17979.
5. Giannozzi, P.; Baroni, S.; Bonini, N.; Calandra, M.; Car, R.; Cavazzoni, C.; Ceresoli, D.; Chiarotti, G. L.; Cococcioni, M.; Dabo, I. et al. Quantum Espresso: A Modular and Open-Source Software Project for Quantum Simulations of Materials. *J.Phys.-Condens.Mat.* **2009**, 21, 1-19.
6. Perdew, J. P.; Zunger, A. Self-Interaction Correction to Density-Functional Approximations for Many-Electron System. *Phys. Rev. B* **1981**, 23, 5048-5079.
7. Carter, D. A.; Pemberton, J. E. Surface-enhanced Raman scattering of the Acid-base forms of Imidazole on Ag. *Langmuir* **1992**, *8*, 1218-1225.
8. Carter, D. A.; Pemberton, J. E. Raman Spectroscopy and Vibrational Assignments of 1 and 2-Methylimidazole. *J. Raman Spectrosc.* **1997**, *28*, 939-946.
9. Colombo, L. Low Frequency Raman Spectrum of Imidazole Single Crystal. *J. Chem. Phys.* **1968**, *49*, 4688-4695.
10. Colombo, L.; Bleckmann, P.; Schrader, B.; Schneider, R.; Plesser, T. Calculation of Normal Vibrations and Intra- and Intermolecular Force Constants in Crystalline Imidazole. *J. Chem. Phys.* **1974**, *61*, 3270-3278.
11. Loeffen, P. W.; Pettifer, R. F.; Fillaux, F.; Kearley, G. J. Vibrational Force Field of Solid Imidazole from Inelastic Neutron Scattering. *J. Chem. Phys.* **1995**, *103*, 8444-8455.
12. Majoube, M.; Vergoten, G. Lattice Vibrations of Crystalline Imidazole and ^{15}N and D Substituted Analogs. *J. Chem. Phys.* **1982**, *76*, 2838-2847.
13. Markham, L. M.; Mayne, L. C.; Hudson, B. S.; Zgierski, M. Z. Resonance Raman Studies of Imidazole, Imidazolium, and Their Derivatives: The Effect of Deuterium Substitution. *J. Phys. Chem.* **1993**, *97*, 10319-10325.
14. Perchard, C.; Novak, A. Far-Infrared Spectra and Hydrogen-Bond Frequencies of Imidazole. *J. Chem. Phys.* **1968**, *48*, 3079-3084.
15. Sadlej, J.; Jaworski, A.; Miaskiewicz, K. A Theoretical Study of the Vibrational Spectra of Imidazole and its Different Forms. *J. Mol. Struct.* **1992**, *274*, 247-257.
16. Saini, G. S. S.; Kaur, S.; Tripathi, S.K.; Dogra, S. D.; Abbas, J. M.; Mahajan, C.G. Vibrational Spectroscopic and Density Functional Theory Studies of Chloranil-Imidazole Interaction. *Vib. Spectrosc.* **2011**, *56*, 66-73.
17. Shiau, G. T.; Walter, J. L.; King, S. S. T. Lattice Vibrations of Imidazole Crystals. *Spectrosc. Lett.* **1975**, *8*, 459-473.
18. Wang, G.; Shi, J.; Yang, H.; Wu, X.; Zhang, Z.; Gu, R.; Cao, P. Surface-Enhanced Raman Scattering of Imidazole Adsorbed on an Iron Surface. *J. Raman. Spectrosc.* **2002**, *33*, 125-130.
19. Paliwoda, D.; Dziubek, K. F.; Katrusiak, A. Imidazole Hidden Polar Phase. *Cryst. Growth Des.* **2012**, *12*, 4302-4305.

Figure Caption

Figure 9. Frequency Vs Pressure in the spectral region (a) 150-200 cm^{-1}, (b) 200-1250 cm^{-1}, (c) 1400-1700 $cm^{-1}$and (d) 3000-3300 cm^{-1}, eyes are drawn as a guide to the eyes; circles and stars indicate symmetric and antisymmetric stretching (C2-H2/C3-H3) modes respectively.

Figure 10. *Ab-initio* calculated values of lattice parameters and unit cell volume as a function of pressure; Here solid filled symbols represent calculated values; open symbols are from experimental data of Paliwoda *et al.* [19]; lines are drawn as a guide to the eyes.

Table 2: Raman modes in the lattice region at ambient conditions and 10 GPa.

Observed at 0.1 MPa (cm^{-1})*	Modes at 10 GPa (cm^{-1})	Possible Assignment[12]	Reference[12]
148	282	Hydrogen bonding chain	153
143	227	-	148
112	196	Hydrogen bond bending	114
91/78	177	Hydrogen bond bending	91/78
42/55	150	Hydrogen bond stretching	45/55

*Ambient spectrum was recorded using triple stage T64000 spectrograph while high pressure spectra were recorded using single stage HR460 spectrograph

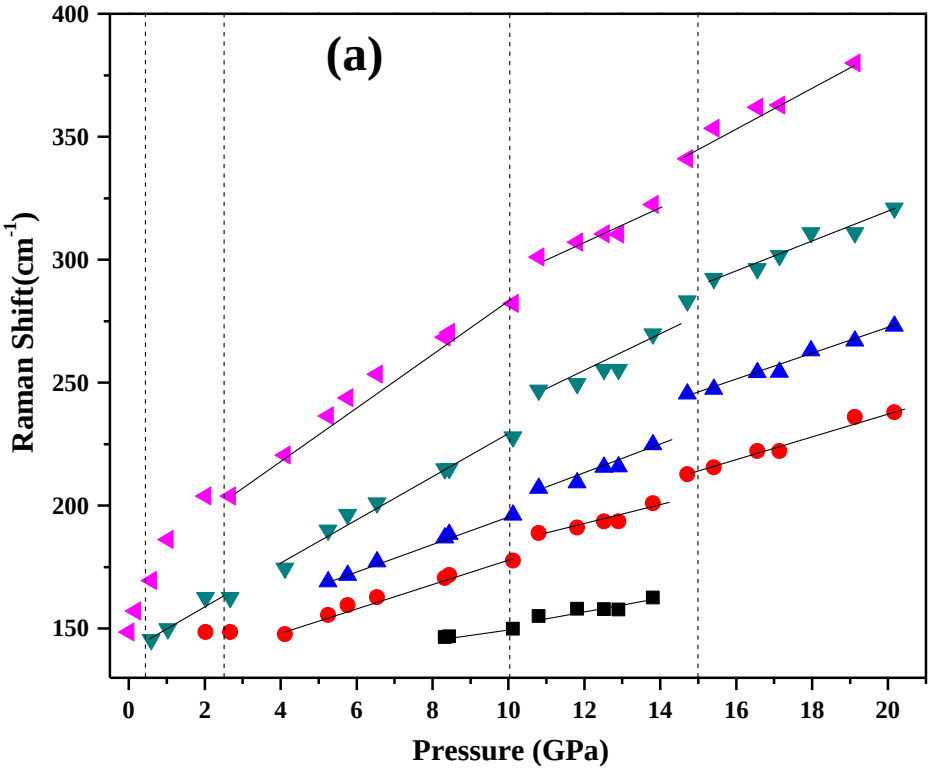
(a)
Raman Shift(cm-1)
Pressure (GPa)
400
350
300
250
200
150
0
2
4
6
8
10
12
14
16
18
20

Figure 9

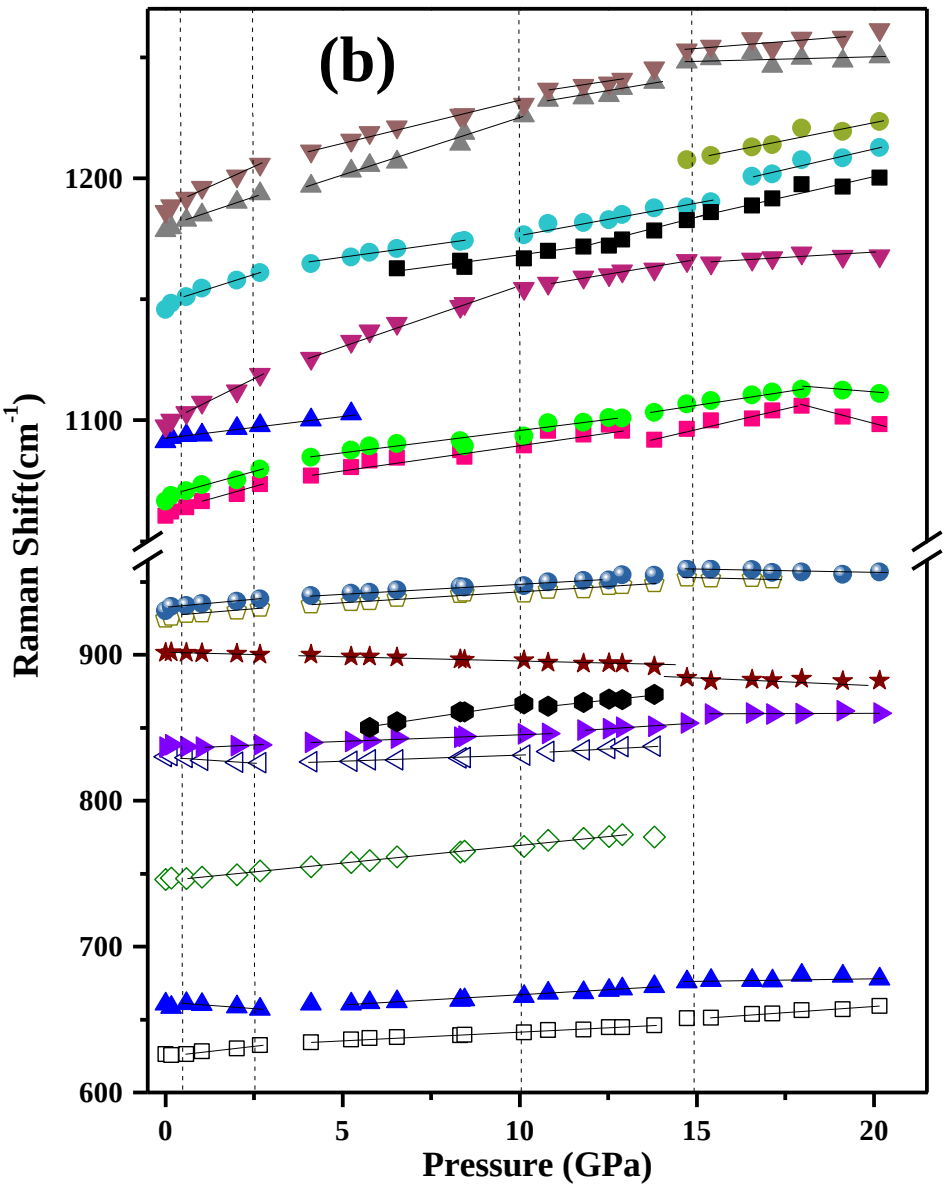
(b)
Raman Shift(cm-1)
1200
1100
900
800
700
600
0
5
10
15
20
Pressure (GPa)

Figure 9

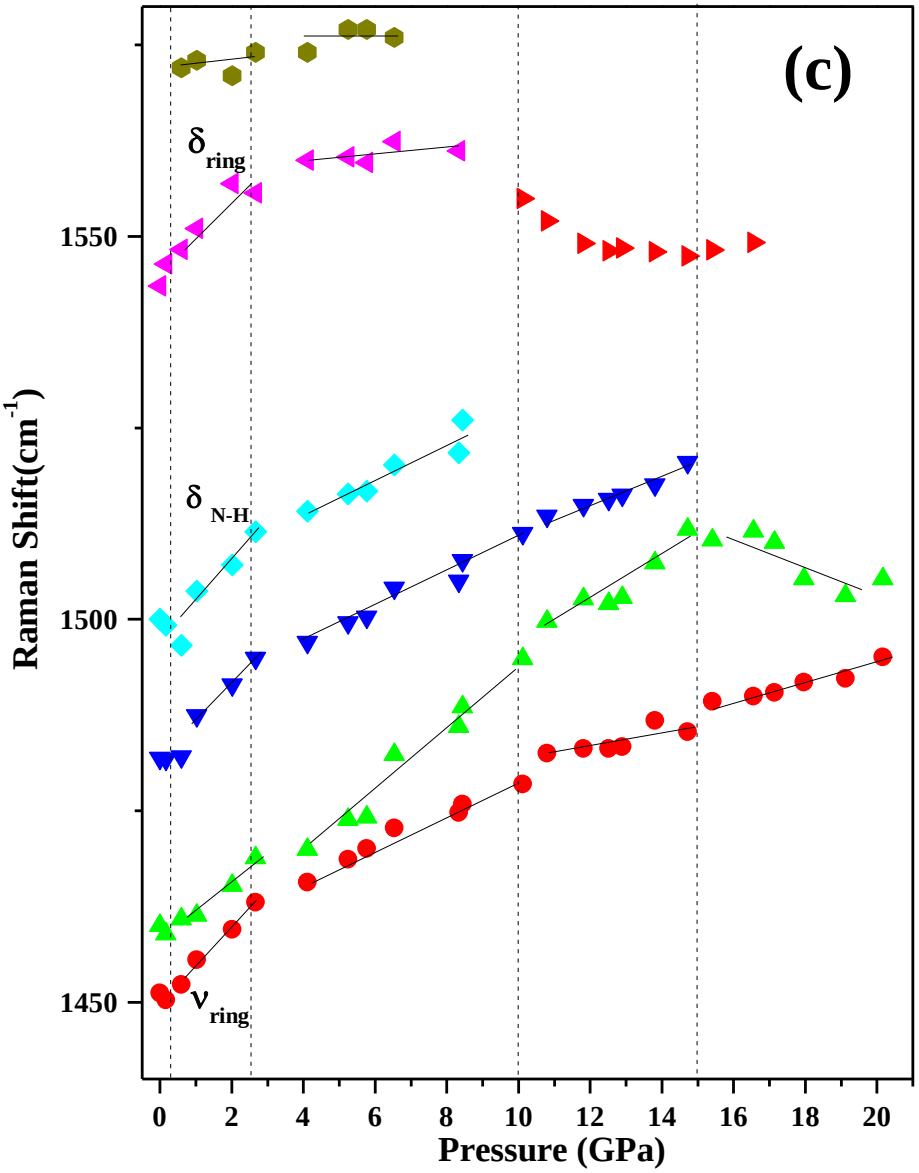
(c)
δ ring
δ N-H
ν ring
1550
1500
1450
Raman Shift(cm-1)
0
2
4
6
8
10
12
14
16
18
20
Pressure (GPa)

Figure 9

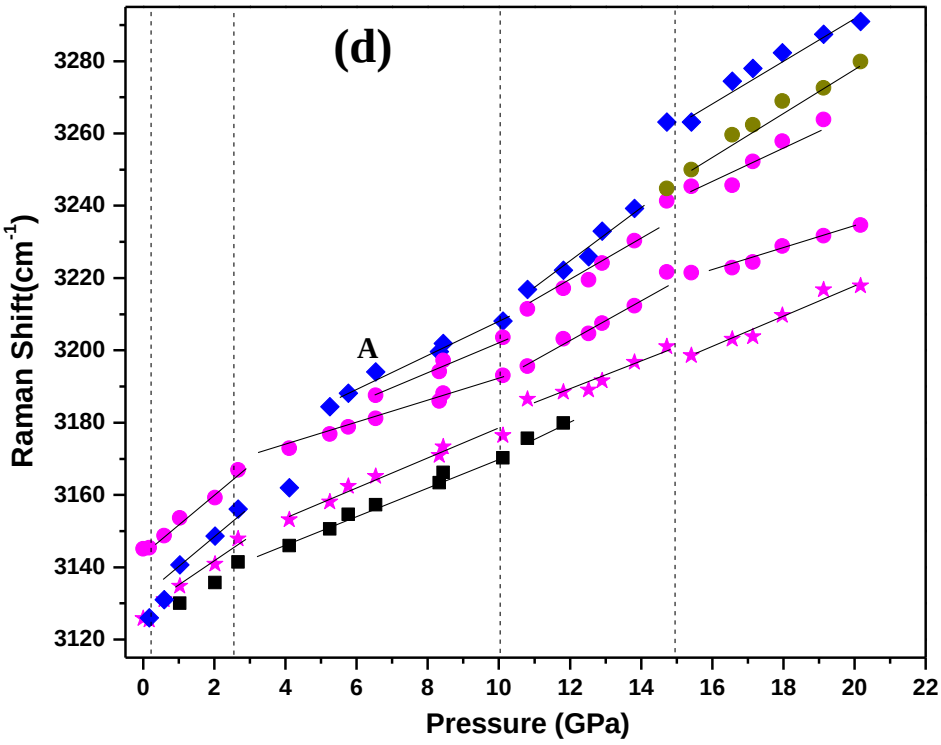
(d)
A
Raman Shift(cm-1)
Pressure (GPa)
3280
3260
3240
3220
3200
3180
3160
3140
3120
0
2
4
6
8
10
12
14
16
18
20
22

Figure 9

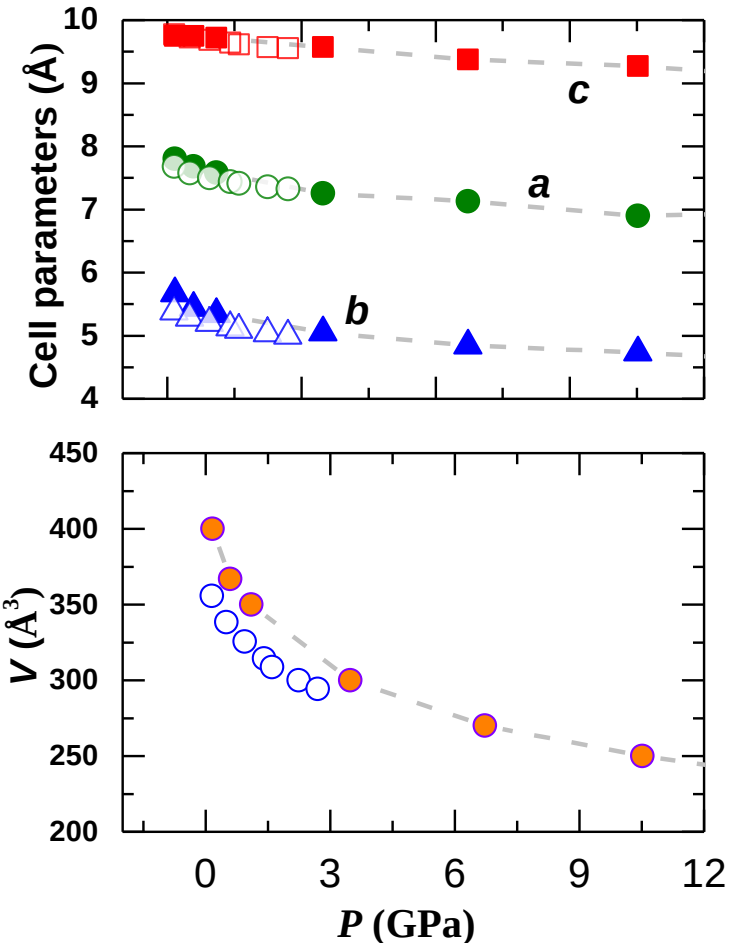
Cell parameters (Å)
10
9
8
7
6
5
4
c
a
b
450
400
350
300
250
200
V (Å3)
0
3
6
9
12
P (GPa)

Figure 10